Journal Pre-proofs

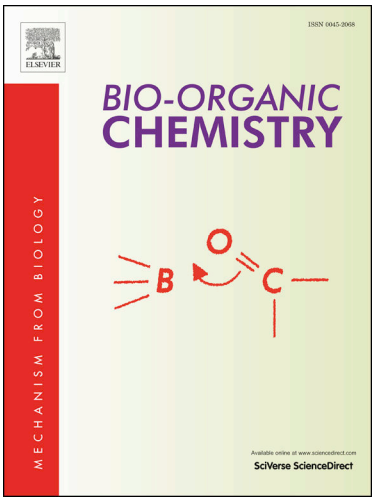

Exploiting the 4-hydrazinobenzoic acid moiety for the development of anti-cancer agents: synthesis and biological profile

Hatem A. Abuelizz, Hanem M. Awad, Mohamed Marzouk, Fahd A. Nasr, Ahmed H. Bakheit, Ahmed M. Naglah, Nasser S. Al-shakliah, Rashad Al-Salahi

PII: S0045-2068(20)31395-X
DOI: https://doi.org/10.1016/j.bioorg.2020.104098
Reference: YBIOO 104098

To appear in: *Bioorganic Chemistry*

Received Date: 25 March 2020
Revised Date: 26 May 2020
Accepted Date: 10 July 2020

Please cite this article as: H.A. Abuelizz, H.M. Awad, M. Marzouk, F.A. Nasr, A.H. Bakheit, A.M. Naglah, N.S. Al-shakliah, R. Al-Salahi, Exploiting the 4-hydrazinobenzoic acid moiety for the development of anticancer agents: synthesis and biological profile, *Bioorganic Chemistry* (2020), doi: https://doi.org/10.1016/j.bioorg.2020.104098

Exploiting the 4-hydrazinobenzoic acid moiety for the development of anticancer agents: synthesis and biological profile

Hatem A. Abuelizz[a], Hanem M. Awad[b], Mohamed Marzouk[b], Fahd A. Nasr[c], Ahmed H. Bakheit[a,d] , Ahmed M. Naglah[e,f] , Nasser S. Al-shakliah [a], Rashad Al-Salahi[*a]

[a] Department of Pharmaceutical Chemistry, College of Pharmacy, King Saud University, PO Box 2457, Riyadh 11451, Saudi Arabia.

[b] Department of Tanning Materials and Leather Technology, National Research Centre, 33 El-Bohouth St. (Former El-Tahrir St.), Dokki, Cairo 12622, Egypt.

[c] Medicinal Aromatic, and Poisonous Plants Research Center, College of Pharmacy, King Saud University, PO Box 2457, Riyadh, 11451, Saudi Arabia.

[d] Department of Chemistry, Faculty of Science and Technology, El-Neelain University, P.O. Box 12702, Khartoum 11121, Sudan.

[e] Department of Pharmaceutical Chemistry, Drug Exploration and Development Chair (DEDC), College of Pharmacy, King Saud University, Riyadh 11451, Saudi Arabia.

[f] Peptide Chemistry Department, Chemical Industries Research Division, National Research Centre, 33 El-Bohouth St. (Former El-Tahrir St.), Dokki, Cairo 12622, Egypt.

[*] Corresponding author. E-mail: ralsalahi@ksu.edu.sa (R.Al-Salahi).

ABSTRACT

Thirteen 4-hydrazinobenzoic acid derivatives were elaborated and characterized by spectral analyses (NMR and MS). Evaluation of their *in vitro* cytotoxic activity showed that some of the targets demonstrated potent inhibitory effects against HCT-116 and MCF-7 cancer cells. The IC_{50} values ranged between 21.3 ± 4.1 and 28.3 ± 5.1 µM, respectively, whereas those of doxorubicin (reference drug) ranged between 22.6 ± 3.9 and 19.7 ± 3.1 µM, respectively. The active targets **6**, **7** and **9** exhibited very weak cytotoxicity on normal cells (RPE-1) and showed higher IC_{50} values against HCT-116 and MCF-7 cells in comparison to doxorubicin. Furthermore, compounds **7, 9** and **10** inhibited the proliferation of MCF-7 by the induction of apoptosis. The bioassay results in the regression plots generated in 3D QSAR models were in agreement and correlated with the anticancer results

of the target molecules. The 4-hydazinobenzoic acid derivatives can be used as cornerstones for further structural modifications as future anticancer agents.

Keywords: 4-Hydrazinobenzoic acid, MTT assay, Anticancer, Apoptosis, 3D QSAR

1. Introduction

The development of chemotherapeutic agents is a fascinating challenge in the field of pharmaceutical chemistry because cancer remains the most frequent cause of mortality, particularly in the developed world. [1-5]. Currently, several anticancer agents (either alone or in combination) have limited activity and their response rates still largely unimproved in clinical trials. Although there have been major advances in chemotherapeutic therapy and much has been done to study the biology of cancer, the goal of overcoming this malignancy is a distant reality. Nowadays, most available chemotherapeutic agents are non-selective; thus, exert their activities against both cancer and normal cells, specifically those that rapidly proliferate. In addition, they have undesired toxic side effects. Thus, the similarity between normal and cancer cells remains the main hurdle to the development of an ultimate anticancer remedy [6-8].

Hydrazinobenzoic acid is a building block for the construction of many heterocyclic compounds with a variety of pharmacological properties. For instance, 2-hydrazinobenzoic acid reacted with *N*-cyanoimido(dithio)carbonates to afford 2-alkyloxy(thioalky)-[1,2,4]triazolo[1,5-*a*]quinazolines. Some of the 1,2,4-triazoloquinazolines were found as potent adenosine antagonist, antidiabetic, antioxidant, antihypertensive, antimicrobial, antihistamine, and anti-inflammatory agents [9-16]. The 5-choro-[1,2,4]triazolo quinazolines showed promising cytotoxicity against HepG2, melanoma (SK-MEL28), and medulloblastoma (Daoy) cell lines [1]. A new series of 5-hydrazono-[1,2,4]triazolo[1,5-*a*]quinazolines demonstrated potent anticancer activity against HeLa L929, MCF-7, and Hep-G2 cells [7]. The novel bis-triazolo[1,5-*a*:4,3-*c*]quinazoline and 5-ethoxy-[1,2,4]triazoloquinazoline were found to possess the highest cytotoxic effects against HCT-116 and HepG2 carcinoma cells [17]. In our previous work, we incorporated a 4-hydrazinobenzoic acid moiety with the triazole pharmacophore to afford the novel 1,2,4-triazolebenzoic acid hybrid scaffolds with potent antiproliferative activity against HCT-116 and MCF-7 human cancer cells [4].

Considering the above facts and continuing our ongoing research dealing with the chemistry of hydrazinobenzoic acid to elaborate new anticancer agents. The incorporation of pharmacophoric templates into one molecule can have positively enhanced chemotherapeutic potential [2, 4]. Herein, we incorporated 4-hydrazinobenzoic acid (**1**) as free base with several isothiocyanates, aldehydes, and acid anhydrides to generate the target compounds (**2**–**13**). Thereafter, their *in vitro* cytotoxicity was evaluated against MCF-7 and HCT-116 cancer cell lines and normal human RPE-1 cells as well.

2. Results and discussion

2.1. Chemistry

4-Hydrazinobenzoic acid hydrochloride was added in portions to a stirred solution of dimethyl-*N*-cyanoimidodithiocarbonate to derive 4-hydrazinobenzoic acid as a free base in yield of 45% and 4-(5-amino-3-(methylthio)-1,2,4-triazol-1-yl) benzoic acid. The later structure was confirmed, characterized, and evaluated in our previous paper [4]. The free base of 4-hydrazinobenzoic acid (**1**) was used as the starting material to produce the targets **2**–**11** and **13** (Scheme 1). The reaction of **1** with several aldehydes afforded the hydrazones **2**–**4** in a good yield. Whereas the hydrazinecarbothioamide derivatives **5**–**10** were obtained from the reaction of **1** with different isothiocyanates, and the corresponding compounds **11** and **13** were resulted upon the treatment of **1** with appropriate acid anhydrides (Scheme 1). Compound **12** was previously reported and characterized [18]. The chemical structures of the compounds **1**–**11** and **13** were established by NMR and HREI-MS analyses (see experimental data) and the aid of comparison with structural related compounds in literature [4].

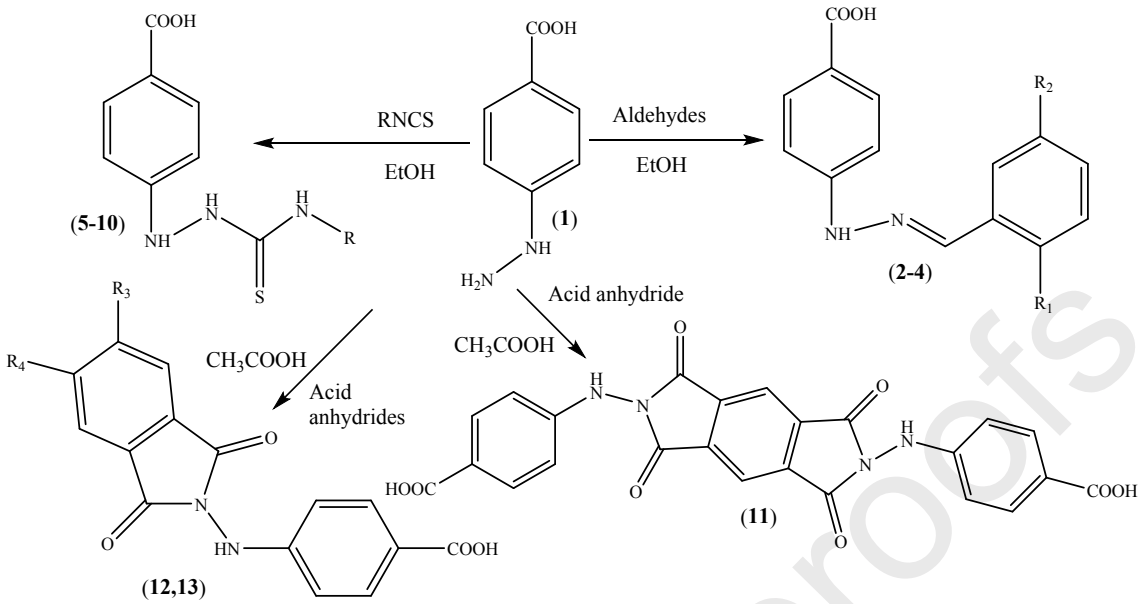

R_1: OH, R_2: methyl **(2)**; R_1: OH, R_2: methoxy **(3);** R_1: OH, R_2: nitro **(4)**; R: methyl **(5)**; R: ethyl **(6)**; R: allyl **(7);** R: butyl **(8)**; R: benzyl **(9); R:** phenethyl **(10)**; R_3 &R_4: H **(12)**; R_3 &R_4: Cl **(13).**

Scheme 1. Main synthetic routes for compounds **2**-**13**

2.2. Biology

The targets **1**–**13** were evaluated for their cytotoxicity using the MTT assay. In the form of % cell viability, the *in vitro* cytotoxic activity was determined against two cancer cell lines (HCT-116 and MCF-7) and one normal cell line (RPE-1) in relative to doxorubicin as the reference drug. As shown in Figures 1–3, all targets suppressed the cell lines in a dose-dependent manner. A comparison study between the cytotoxic effect of each compound and that of doxorubicin was performed to determine the efficacy of synthesized products **1**–**13**. Table 1 shows that compounds **7** and **10** (IC_{50} = 21.3 ± 4.1 and 21.8 ± 4.1 μM) had significantly more potent cytotoxicity than doxorubicin (IC_{50} = 22.6 ± 3.9 μM) against HCT-116 cells. However, compounds **6**, **8** and **9** (IC_{50} = 25.6 ± 4.4, 24.1 ± 4.2 and 24.5 ± 4.9 μM) exhibited good activity. In case of human MCF-7 cells, compounds **2**, **4, 7, 9** and **10** (IC_{50} = 24.4 ± 2.9, 24.5 ± 4.6, 25.0 ± 4.6, 26.0 ± 4.3, and 23.5 ± 4.9 μM, respectively) showed high cytotoxicity compared to that of doxorubicin (IC_{50} = 19.7 ± 3.1 μM). However, compounds **1**, **3** and **13** (IC_{50} = 34.6 ± 6.3, 30.9 ± 5.3 and 30.9 ± 5.6 μM) had slightly less cytotoxic effects.

In case of RPE-1 cells, compounds **3**, **4**, **8**, **10** and **12** (IC_{50} = 60.8 ± 11.3, 56.2 ± 9.5, 62.3 ± 14.5, 62.5 ± 14.1 and 58.0 ± 11.9 μM) were more cytotoxic than doxorubicin (IC_{50} = 64.0 ± 13.2 μM), whereas **13** (IC_{50} = 64.2 ± 13.3 μM) was as cytotoxic as doxorubicin. Additionally, the targets **6**, **7** and **9** (IC_{50} = 85.7 ± 15.8, 75.2 ± 15.3 and 96.0 ± 17.5 μM) demonstrated significantly less cytotoxic effects against RPE-1 cells and the remaining compounds had slightly less cytotoxicity

Table 1. IC_{50} values of the target compounds according to the MTT assay

Cps	IC_{50} (μM) ± SD			Therapeutic Index (TI)	
	HCT-116	MCF-7	RPE-1	HCT-116	MCF-7
1	34.6 ± 5.9	34.6 ± 6.3	67.2 ± 12.5	1.9	1.9
2	31.2 ± 4.1	24.4 ± 2.9	66.8 ± 14.1	2.1	2.7
3	38.9 ± 5.9	30.9 ± 5.3	60.8 ± 11.3	1.6	2.0
4	29.3 ± 5.1	24.5 ± 4.6	56.2 ± 9.5	1.9	2.3
5	29.9 ± 4.6	29.7± 5.5	67.6 ± 14.7	2.3	2.3
6	25.6 ± 4.4	28.3 ± 5.1	85.7 ± 15.8	3.3	3.0
7	21.3 ± 4.1	25.0 ± 4.6	75.2 ± 15.3	3.5	3.0
8	24.1 ± 4.2	26.2 ± 4.3	62.3 ± 14.5	2.6	2.4
9	24.5 ± 4.9	26.0 ± 4.3	96.0 ± 17.5	3.9	3.7
10	21.8 ± 4.1	23.5 ± 4.9	62.5 ± 14.1	2.9	2.7
11	28.0 ± 4.1	26.3 ± 4.9	66.3 ± 13.1	2.4	2.5
12	33.3 ± 4.5	28.2 ± 5.3	58.0 ± 11.9	1.7	2.1
13	32.5 ± 5.1	30.9 ± 5.6	64.2 ± 13.3	2.0	2.1
Doxorubicin	22.6 ± 3.9	19.7 ± 3.1	64.0 ± 13.2	2.8	3.3

The therapeutic index (TI) was calculated to determine the safety of each compound according to the following equation: (**TI** = IC_{50} in the normal cells / IC_{50} in the cancer cells). As illustrated in Table 1, for MCF-7 cells, compound **9** had a higher TI (3.7) than doxorubicin (3.3); however, compounds **2**, **6**, **7** and **10** had a slightly lower TIs than doxorubicin, whereas **1**, **3–5, 8** and **11- 13** had lower TIs than doxorubicin.

In case of HCT-116 cells, compounds **6, 7, 9,** and **10** had higher TIs (3.3, 3.5, 3.9 and 2.9, respectively) than doxorubicin (2.8); **8** had slightly lower TI (2.6) than doxorubicin; **1–5** and **11-13** had significantly less TIs than the reference drug. This suggests that **6**, **7, 9** and **10** are more active anticancer candidate drugs against two human cancer cells in regard to their safety and efficacy. Moreover, the results indicated that the targets **1**–**13** demonstrated weak to high cytotoxicity against MCF-7 and HCT-116 cell lines with IC_{50} values ranging in 23.5 ± 4.9 to 34.6 ± 6.3 and 21.3 ± 4.1 to 38.9 ± 5.9 µM, respectively (Table 1). The insertion of isothiocyanate group significantly increased cytotoxicity as revealed by compounds **6**, **7, 9** and **10,** which demonstrated significant TI values that ranged between 2.7 and 3.9 against both cancer cell lines.

The condensation products with aldehydes (**2–4)** increased cytotoxicity in MCF-7 cells, but did not increase cytotoxicity in HCT-116 cells as revealed by the structure-activity relationship study The parent compound **1** showed the same activity against both cancer cells; however, its transformed products **2**, **5–11**, **13** displayed higher activity against MCF-7 and HCT-116 cells, respectively. In addition, compounds **3** and **12** exhibited a lower activity against HCT-116 cells than **1**. We noticed that the type of isothiocyanate in compounds **5–10** and acid anhydride in **11–13** displayed varying cytotoxicity profiles (Table 1).

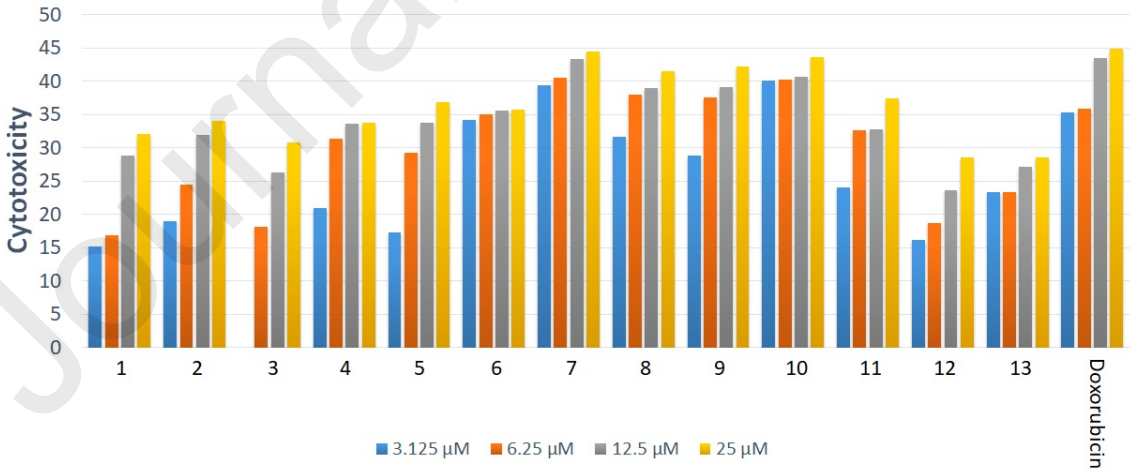

Fig. 1. Dose dependent cytotoxic activities of compounds **1-13** against HCT-116 cancer cells

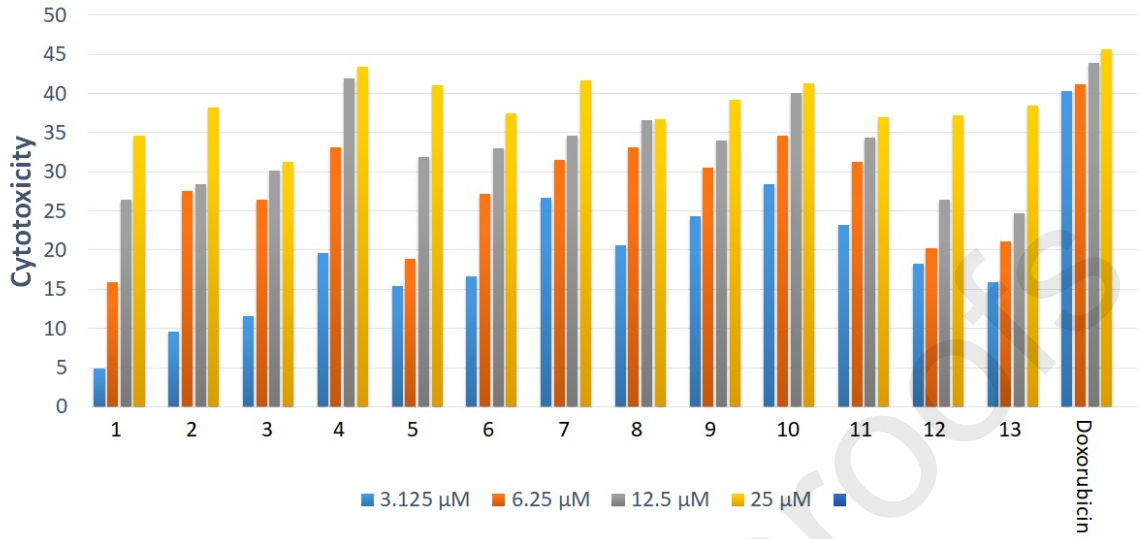

Fig. 2. Dose dependent cytotoxic activities of compounds **1-13** against MCF-7 cancer cells

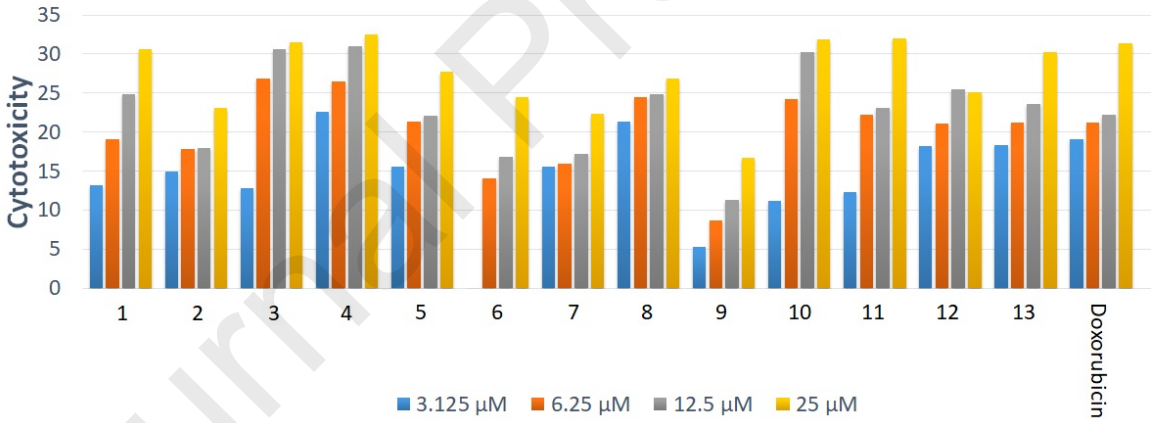

Fig. 3. Dose dependent cytotoxic activities of compounds **1-13** against RPE-1 normal cells

2.3. Apoptosis detection

To provide more evidence for the anticancer effect of promising compounds, Hoechst 33258 staining was carried out to investigate the nuclear morphological changes following compound treatment on MCF-7 cells. Control cells without treatment exhibited uniformly light blue staining and intact cell membranes (Fig. 4). In contrast, cells treated with the IC_{50} of each compound for 24 h were low in numbers and stained bright blue because of chromatin condensation. Moreover, quantitative analysis of the apoptotic effects of the

compounds on MCF-7 cells was conducted by flow cytometry using Annexin V-FITC and PI double staining, which detect the phosphatidylserine externalization, as a consequence of the initiation of apoptosis. After treatment with compounds **7, 9** and **10** (IC_{50} = 25, 26, and 23.5 μM, respectively) for 24 h, the percentage of cells undergoing early apoptotic events was significantly increased from 1.2 ± 0.5 % of the control to 17.3 ± 1.6, 10.1 ± 1.2 %, and 6.3 ± 0.9, for compounds **7**, **9,** and **10,** respectively. In the same manner, the percentage of late apoptotic cells were increased to 3.6 ± 0.3 %, 3.1 ± 0.1 % and 5.9 ± 0.4 % for compounds **7**, **9**, and **10**, respectively in compare to control. However, no significant differences were reported in the percent of necrotic deaths for all tested compounds which indicated that induction of cell apoptosis reflected the antitumor effect of the compounds (Fig. 5).

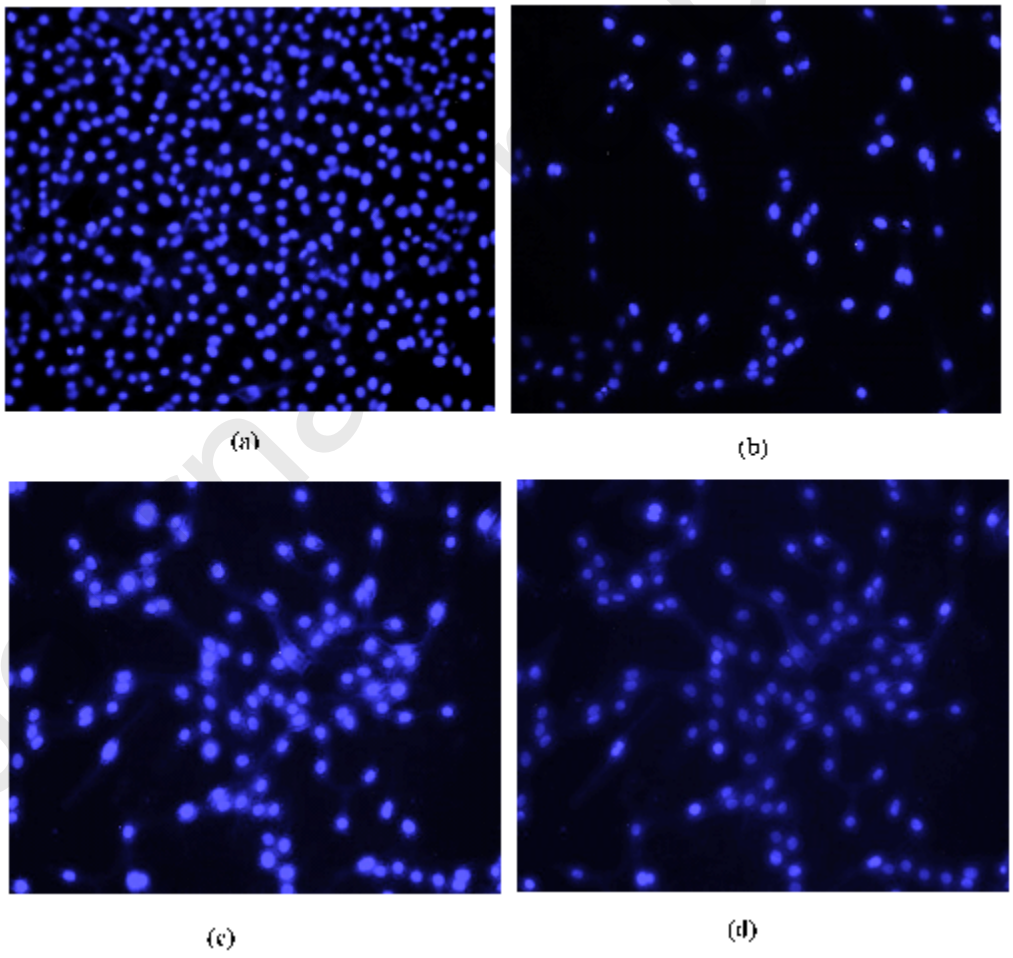

Fig. 4. Fluorescent images of Hoechst 33258 staining showing induced cell death. (a) MCF-7 cells without treatment served as a control, (b-d) cells were treated for 24 h prior to Hoechst staining compounds **7**, **9** and **10** (25, 26 and 23.5, μM, respectively).

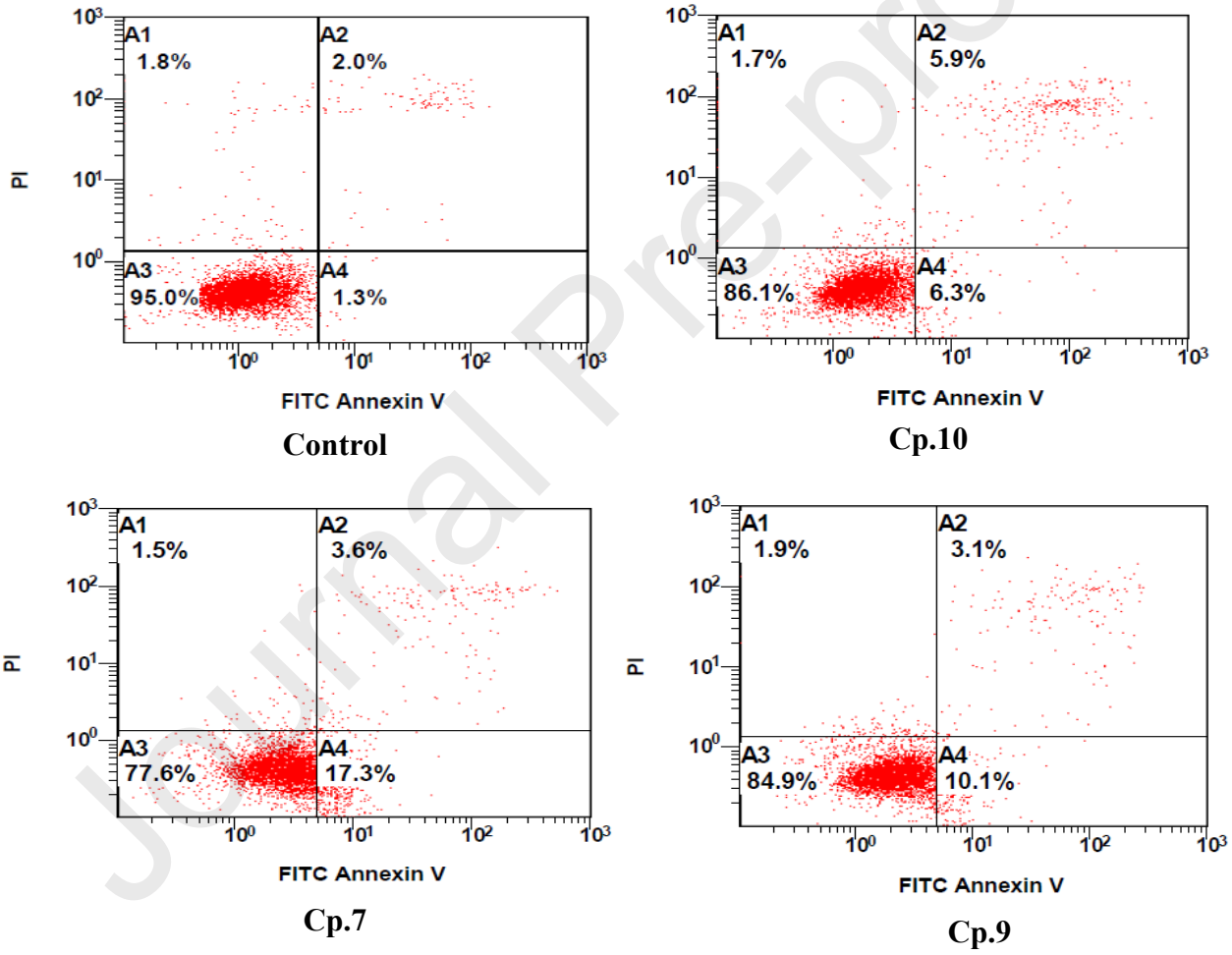

Fig. 5. Compounds treatment induces apoptosis in MCF-7 cells**.** MCF-7 cells were treated with compounds **7, 9** and **10** (25, 26 and 23.5 μM, respectively) for 24 h, then stained with Annexin

V-FITC/PI, and apoptosis was quantified using FACS analysis. Each quadrant represents cells in different stages; A3 viable, A4 early apoptosis, A2 late apoptosis, and A1 necrosis.

2.4. 3D QSAR analysis

Employing discovery Studio 4.5 to build 3D QSAR models of 4-hydrazinobenzoic acid derivatives (**1**–**13**) based on their preliminary cytotoxicity results. The calculated pTI values of the target compounds ranged between 5.45080 and 5.58846 (Table S1). The model dataset was built with thirteen compounds with TIs that ranged from 1.6 to 3.9 (Table 1). The pTI values were determined from corresponding TI values using the formula in the following equation: **pTI = -log TI.**

Discovery Studio 4.5 was divided the compounds in the preliminary set into a training set and test set. For a perfect model of QSAR, the value of training set regression coefficient (R^2) and test set regression coefficient (Q^2) should be higher than 0.6 and 0.5, respectively. In our study, the observed R^2 comparable to the predicted training set response was 0.9352 and 0.9122, whereas the Q^2 comparison of the test set was 0.6759 and 0.6696 for HCT-116 and MCF-7, respectively (Table 2S), which illustrated the acceptability of the QSAR model. Figure 6 displays the plot of the pTI observed results compared to the predicted results. The predicted pTI value and residual error of the thirteen compounds for that QSAR model are summarized in Table S1. In addition, the iso-surfaces aligned compounds of the 3D-QSAR model coefficients on van der Waals grids (Fig. 7b &d) and electrostatic potential grids (Fig. 7a &c) are listed for HCT-116 and MCF-7 respectively. In the electrostatic map, negative charge (high electron density) is sited in red contour regions expecting high activity and partial positive charge (low electron density) is sited in blue contour expecting high activity. In addition, in the steric map, the steric bulk areas (activity) increase when the green contour is increased or yellow contour is decreased. In the maps, the activity of the compounds increases with the increase in the positive charge and decrease in the volume of compound as shown in Figure 7a–d. The summarized data demonstrate that compound **9**, the most potent antiproliferative agent (TI against HCT-116 = 3.9 and against MCF-7 = 3.7), has a benzylisothiocyanate substituent that could be

displayed a pivotal role in cytotoxicity profile. The 3D QSAR models fit the cytotoxic activity well, which provides knowledge for further modification.

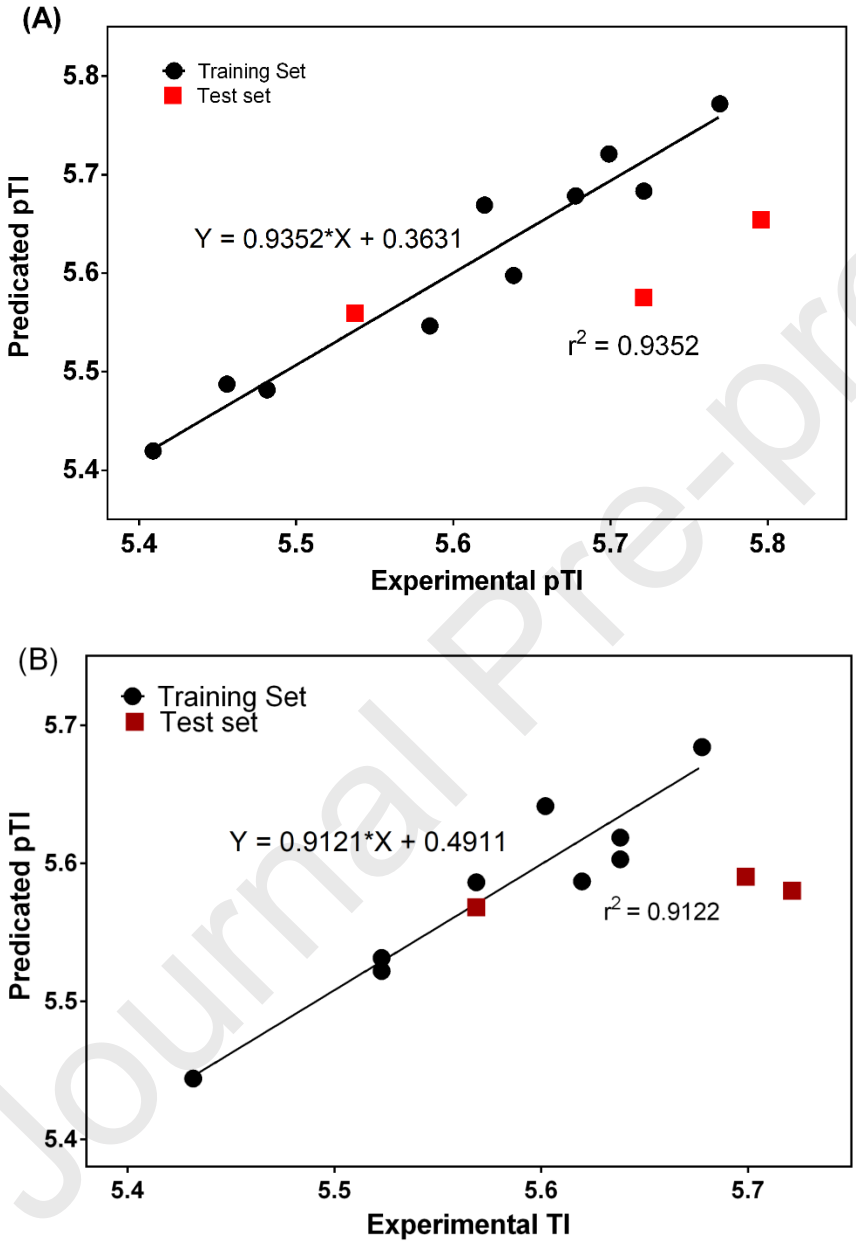

Fig. 6. Plot of experimental versus predicted **(a)** a human colon cancer and **(b)** a breast cancer therapeutic index activities of training set and test set.

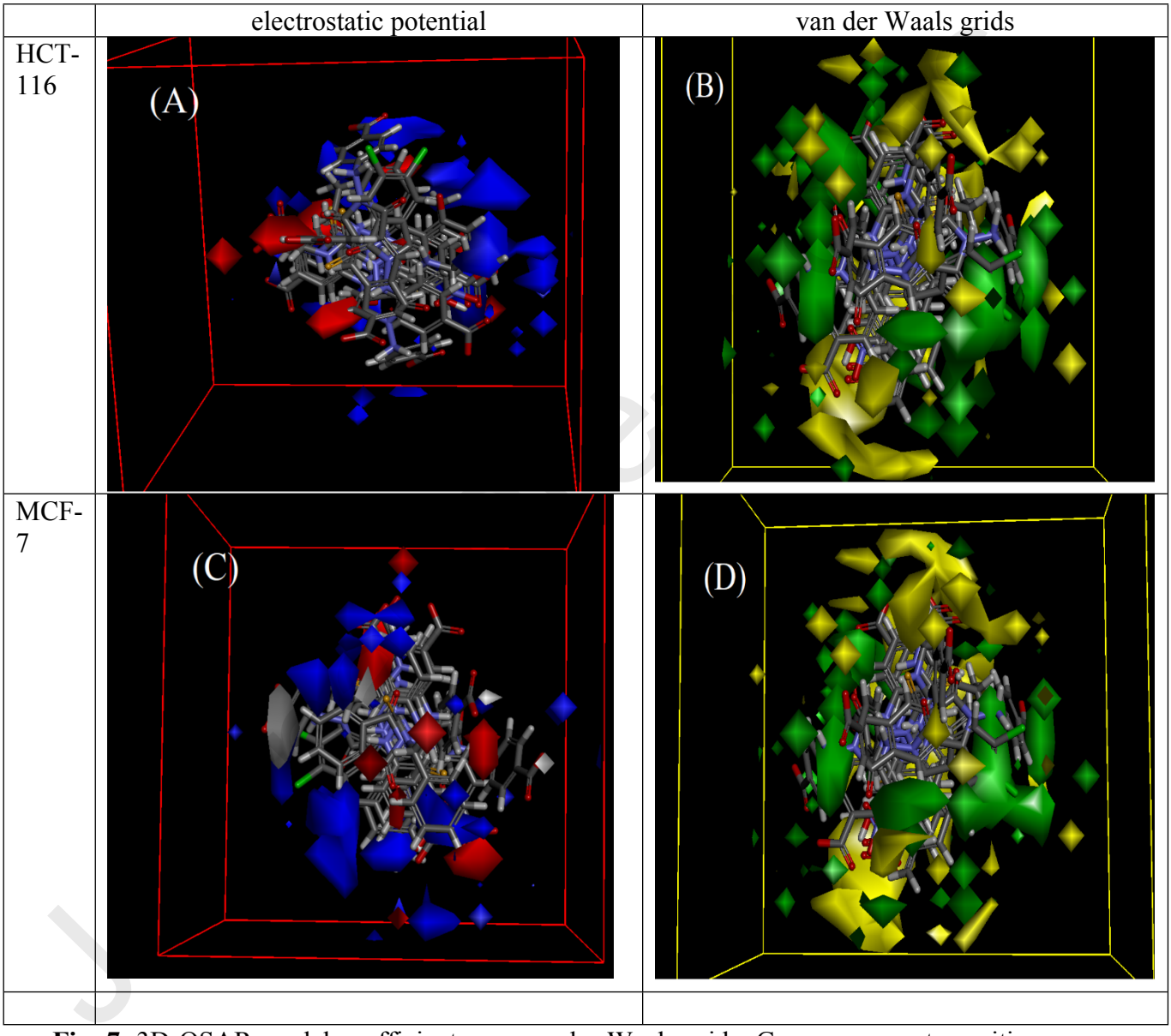

Fig. 7. 3D-QSAR model coefficients on van der Waals grids, Green represents positive coefficients, yellow represents negative coefficients, (b) and (d). 3D-QSAR model coefficients on electrostatic potential grids, Blue represents positive coefficients, red represents negative coefficients, (a) & (c). For HCT-116, (a) & (b) and for MCF-7, (c) & (d).

3. Conclusions

A series of 4-hydrazinobenzoic acid compounds were evaluated for their *in vitro* cytotoxicity against MCF-7 and HCT-116 human cancer cell lines. The study revealed that targets **6**, **7**, **9** and **10** demonstrated potent antiproliferative effects. The incorporation of an isothiocyanate moiety into the 4-hydrazinobenzoic acid platform enhanced cytotoxicity. The targets **6**, **7** and **9** not only exhibited promising cytotoxicity against the tested cancer cells, but showed very weak cytotoxic effects in normal cells, which implies that these can be used as candidates for anticancer therapy. Moreover, compounds **7**, **9** and **10** showed antiproliferative activity by inducing apoptosis in MCF-7 cancer cells; thus, they are worthy of further research for the development of novel anticancer drugs. In 3D QSAR analysis, the predicted pTI values of the active compounds showed a significant correlation with the experimental values from the generated regression and principal component analysis plots. These discoveries strongly support the cytotoxicity results of compounds **6, 7, 9** and **10**.

4. Experimental

4.1. Chemistry

It is worth mentioning that the registration CAS numbers for the products **1–10** had already been assigned. However, their chemical properties, and structural characterization are not available in literature. In a basic medium, the free base **1** was resulted from addition of 4-hydazinobenzoic acid HCl (1.1 mmol) in a portion-wise to stirred solution of dimethyl-*N*-cyanoimidodithiocarbonate (1 mmol) in boiling ethanol (15 mL). A mixture of **1** (1.4 mmol) and aldehyde (1.5 mmol) or an appropriate isothiocyanate (1.5 mmol) was heated in ethanol (15 mL) for 5-8 h. After cooling, the solid was filtered off, washed with water and dried to afford the final products **2-10.** When the parent **1** (2 or 1 mmol) was allowed to react under reflux condition with pyromellitic dianhydride (1.1 mmol) or 4,5-dichlorophthalic anhydride (1.1 mmol) in glacial acetic acid (10 mL) for 15 h, the corresponding **11** and **13** were obtained after treatment the boiling solution with ice water.

4.1.1. 4-Hydrazinylbenzoic acid (1)

CAS number: 619-67-0; pale yellow amorphous powder (45%); mp 222–224 °C; ^{1}H NMR (700 MHz, DMSO-d_6): δ 12.38 (br s, 1H, -COOH), 9.46, 8.45 (each br s, 2H, -NH-CS-NH-), 8.24 (m, 1H, Ar-NH), 7.68 (d, J = 7.8 Hz, 2H, H-2/6), 7.51 (s, 1H, -NH), 6.75 (d, J = 7.8 Hz, 2H, H-3/5); ^{13}C NMR (175 MHz, DMSO-d_6): δ 168.1 (C-7), 156.3 (C-4), 131.3 (C-2/6), 117.8 (C-1), 110.3 (C-3/5); HRMS (EI), *m/z* Calcd for C7H8N2O2 $(M)^{\bullet+}$ 152.0586, found 152.0613.

4.1.2. (E)-4-(2-(2-Hydroxy-5-methylbenzylidene)hydrazinyl)benzoic acid (2)

CAS number: 1608619-21-1; white amorphous powder (70%); mp 271–273 °C; ^{1}H NMR (700 MHz, DMSO-d_6): δ 12.33 (br s, 1H, -COOH), 10.83 (br s, 1H, -OH), 10.05 (br s, 1H, -NH), 8.22 (s, 1H, -N=CH-), 7.83 (d, J = 8.2 Hz, 2H, H-2/6), 7.57 (br s, 1H, H-6'), 7.02 (d, J = 8.2 Hz, 2H, H-3/5), 7.00 (br d, J = 8.3 Hz, 1H, H-4'), 6.79 (d, J = 8.2 Hz, 1H, H-3'), 2.25 (s, 3H, Ar-CH_3); ^{13}C NMR (175 MHz, DMSO-d_6): δ 167.6 (C-7), 154.1 (C-2'), 148.9 (C-4), 138.8 (C-7'), 131.8 (C-2/6), 130.9 (C-4'), 128.4 (C-5'), 127.2 (C-6'), 120.7 (C-1), 120.6 (C-1'), 116.3 (C-3'), 111.4 (C-3/5), 20.6 (Ar-CH_3); HRMS (EI), *m/z* Calcd for $C_{15}H_{14}N_2O_3$ $(M)^{\bullet+}$ 270.1004, found 270.1053.

4.1.3. (E)-4-(2-(2-Hydroxy-5-methoxybenzylidene)hydrazinyl)benzoic acid (3)

CAS number: 385406-90-6; white amorphous powder (72%); mp 265–267 °C; ^{1}H NMR (700 MHz, DMSO-d_6): δ 12.33 (br s, 1H, -COOH), 10.86 (br s, 1H, -OH), 9.78 (br s, 1H, -NH), 8.23 (s, 1H, -N=CH-), 7.83 (d, J = 8.8 Hz, 2H, H-2/6), 7.22 (d, J = 2.7 Hz, 1H, H-6'), 7.04 (d, J = 8.8 Hz, 2H, H-3/5), 6.81 (m, 2H, H-3'/4'), 3.74 (s, 3H, OCH_3); ^{13}C NMR (175 MHz, DMSO-d_6): δ 167.7 (C-7), 152.8 (C-2'), 150.3 (C-5'), 148.9 (C-4), 138.1 (C-7'), 131.8 (C-2/6), 121.5 (C-1), 120.8 (C-1'), 117.3 (C-4'), 116.8 (C-3'), 111.4 (C-3/5), 110.4 (C-6'), 55.9 (OCH_3); HRMS (EI), *m/z* Calcd for $C_{15}H_{14}N_2O_4$ $(M)^{\bullet+}$ 286.0954, found 286.1003.

4.1.4. (E)-4-(2-(2-Hydroxy-5-nitrobenzylidene)hydrazinyl)benzoic acid (4)

CAS number: 850186-63-9; yellow amorphous powder (62%); mp 293–295 °C ; ^{1}H NMR (700 MHz, DMSO-d_6): δ 12.38 (br s, 1H, -COOH), 11.64 (br s, 1H, -OH), 11.07 (br s, 1H, -NH), 8.57 (br s, 1H, H-6'), 8.25 (s, 1H, -N=CH-), 8.07 (br d, J = 8.9 Hz, 1H, H-4'),

7.86 (d, J = 8.3 Hz, 2H, H-2/6), 7.09 (d, J = 8.3 Hz, 2H, H-3/5), 7.05 (d, J = 8.9 Hz, 1H, H-3'); ^{13}C NMR (175 MHz, DMSO-d_6): δ 167.7 (C-7), 161.5 (C-2'), 148.7 (C-4), 140.6 (C-7'), 134.5 (C-5'), 131.8 (C-2/6), 125.5 (C-4'), 122.5 (C-1), 121.5 (C-1'), 121.3 (C-3'), 116.9 (C-6'), 111.7 (C-3/5); HRMS (EI), *m/z* Calcd for $C_{14}H_{11}N_3O_5$ $(M)^{\bullet+}$ 301.0699, found 301.0743.

4.1.5. 4-(2-(Methylcarbamothioyl)hydrazinyl)benzoic acid (5)

CAS number: 855294-99-4; white amorphous powder (76%); mp 256–258 °C (DMF); ^{1}H NMR (700 MHz, DMSO-d_6): δ 12.37 (br s, 1H, -COOH), 9.41, 8.44 (each br s, 2H, -NH-CS-NH-), 8.51 (m, 1H, Ar-NH), 7.79 (d, J = 8.7 Hz, 2H, H-2/6), 6.69 (d, J = 8.7 Hz, 2H, H-3/5), 2.80 (s, 3H, -NHCH_3); ^{13}C NMR (175 MHz, DMSO-d_6): δ 182.9 (>C=S), 167.7 (C-7), 152.7 (C-4), 131.3 (C-2/6), 121.4 (C-1), 111.9 (C-3/5), 31.2 (-NH-CH_3); HRMS (EI), *m/z* Calcd for $C_9H_{11}N_3O_2S$ $(M)^{\bullet+}$ 225.0572, found 225.0623.

4.1.6. 4-(2-(Ethylcarbamothioyl)hydrazinyl)benzoic acid (6)

CAS number: 474819-57-3; white amorphous powder (70%); mp 242–244 °C; ^{1}H NMR (700 MHz, DMSO-d_6): δ 12.37 (br s, 1H, -COOH), 9.36, 8.43 (each br s, 2H, -NH-CS-NH-), 8.19 (m, 1H, Ar-NH), 7.79 (d, J = 8.8 Hz, 2H, H-2/6), 6.69 (d, J = 8.8 Hz, 2H, H-3/5), 3.47 (q, J = 7.0 Hz, 2H, H-1'), 1.04 (t, J = 7.0 Hz, 3H, H-2'); ^{13}C NMR (175 MHz, DMSO-d_6): δ 181.9 (>C=S), 167.7 (C-7), 152.7 (C-4), 131.3 (C-2/6), 121.4 (C-1), 112.0 (C-3/5), 38.6 (C-1'), 15.1 (C-2'); HRMS (EI), *m/z* Calcd for $C_{10}H_{13}N_3O_2S$ $(M)^{\bullet+}$ 239.0728, found 239.0773.

4.1.7. 4-(2-(Allylcarbamothioyl)hydrazinyl)benzoic acid (7)

CAS number: 855202-41-4**;** pale yellow amorphous powder (80%); mp 220–222 °C; ^{1}H NMR (700 MHz, DMSO-d_6): δ 12.38 (br s, 1H, -COOH), 9.49, 8.48 (each br s, 2H, -NH-CS-NH-), 8.34 (m, 1H, Ar-NH), 7.79 (d, J = 8.3 Hz, 2H, H-2/6), 6.70 (d, J = 8.3 Hz, 2H, H-3/5), 5.81 (m, 1H, H-2'), 5.03 (m, 2H, H-3'a,3'b), 4.1 (m, 2H, H-1'); ^{13}C NMR (175 MHz, DMSO-d_6): δ 182.5 (>C=S), 167.7 (C-7), 152.6 (C-4), 135.6 (C-2'), 131.3 (C-2/6), 121.4 (C-1), 115.5 (C-3'), 112.0 (C-3/5), 45.9 (C-1'); HRMS (EI), *m/z* Calcd for $C_{11}H_{13}N_3O_2S$ $(M)^{\bullet+}$ 251.0728, found 251.0743.

4.1.8. 4-(2-(Butylcarbamothioyl)hydrazinyl)benzoic acid (8)

CAS number: 475079-88-0; white amorphous powder (70%); mp 239–241 °C; ^{1}H NMR (700 MHz, DMSO-d_6): δ 12.38 (br s, 1H, -COOH), 9.35, 8.42 (each br s, 2H, -NH-CS-NH-), 8.15 (m, 1H, Ar-NH), 7.79 (d, J = 8.6 Hz, 2H, H-2/6), 6.69 (d, J = 8.6 Hz, 2H, H-3/5), 3.44 (t, J = 7.4 Hz, 2H, H-1'), 1.46 (quintet, J = 7.4 Hz, 2H, H-2'), 1.22 (sixtet, J = 7.4 Hz, 2H, H-3'), 0.86 (t, J = 7.4 Hz, 3H, H-4'); ^{13}C NMR (175 MHz, DMSO-d_6): δ 182.1 (>C=S), 167.7 (C-7), 152.7 (C-4), 131.3 (C-2/6), 121.4 (C-1), 112.0 (C-3/5), 43.4 (C-1'), 31.4 (C-2'), 19.8 (C-3'), 14.3 (C-4'); HRMS (EI), *m/z* Calcd for $C_{12}H_{17}N_3O_2S$ $(M)^{\bullet+}$ 267.1041, found 267.1073.

4.1.9. 4-(2-(Benzylcarbamothioyl)hydrazinyl)benzoic acid (9)

CAS number: 509109-88-0**;** white amorphous powder (82%); mp 236–238 °C; ^{1}H NMR (700 MHz, DMSO-d_6): δ 12.39 (br s, 1H, -COOH), 9.56, 8.53 (each br s, 2H, -NH-CS-NH-), 8.76 (m, 1H, Ar-NH), 7.80 (d, J = 8.5 Hz, 2H, H-2/6), 7.27 (m, 4H, H-3'/5', 2'/6'), 7.21 (br t, J = 7 Hz, 1H, H-4'), 6.73 (d, J = 8.5 Hz, 2H, H-3/5), 4.72 (s, 2H, CH_2-7'); ^{13}C NMR (175 MHz, DMSO-d_6): δ 182.9 (>C=S), 167.7 (C-7), 152.7 (C-4), 140.0 (C-1'), 131.3 (C-2/6), 128.5 (C-3'/5'), 127.6 (C-2'/6'), 127.1 (C-4'), 121.4 (C-1), 112.0 (C-3/5), 46.9 (Ar-CH_2); HRMS (EI), *m/z* Calcd for $C_{15}H_{15}N_3O_2S$ $(M)^{\bullet+}$ 301.0885, found 301.0921.

4.1.10. 4-(2-(Phenethylcarbamothioyl)hydrazinyl)benzoic acid (10)

CAS number: 502432-82-8; white amorphous powder (80%); mp 252–254 °C; ^{1}H NMR (700 MHz, DMSO-d_6): δ 12.38 (br s, 1H, -COOH), 9.46, 8.45 (each br s, 2H, -NH-CS-NH-), 8.24 (m, 1H, Ar-NH), 7.80 (d, J = 8.7 Hz, 2H, H-2/6), 7.25 (br t, J = 7.4 Hz, 2H, H-3'/5'), 7.18 (m, 3H, H-2'/6',4'), 6.69 (d, J = 8.7 Hz, 2H, H-3/5), 3.65 (t, J = 7.6 Hz, 2H, H-8'), 2.81 (t, J = 7.6 Hz, 2H, H-7'); ^{13}C NMR (175 MHz, DMSO-d_6): δ 182.2 (>C=S), 167.7 (C-7), 152.6 (C-4), 139.7 (C-1'), 131.3 (C-2/6), 129.1 (C-3'/5'), 128.8 (C-2'/6'), 126.5 (C-4'), 121.5 (C-1), 112.1 (C-3/5), 45.3 (C-8'), 35.3 (C-7'); HRMS (EI), *m/z* Calcd for $C_{16}H_{17}N_3O_2S$ $(M)^{\bullet+}$ 315.1041, found 315.1083.

4.1.11. 4,4'-((1,3,5,7-Tetraoxo-5,7-dihydropyrrolo[3,4-f]isoindole-2,6(1H,3H)diyl)bis-(azane-diyl)) dibenzoic acid (11)

Brown amorphous powder (52%); mp >300 °C; ^{1}H NMR (700 MHz, DMSO-d_6): δ 12.52 (br s, 2H, 2 x -COO<u>H</u>), 9.27 (br s, 2H, 2 x -NH), 8.43 (s, 2H, H-4'/8'), 7.80 (d, J = 8.5 Hz, 4H, H-2/6, 2"/6"), 6.91 (d, J = 8.5 Hz, 4H, H-3/5, 3"/5"); ^{13}C NMR (175 MHz, DMSO-d_6): δ 167.5 (C-7/7"), 165.2 (C-1',3',5',7'), 150.9 (C-4/4"), 135.8 (C-3'a,4'a,7'a,8'a), 131.5 (C-2/6,2"/6"), 122.4 (C-1,1"), 118.9 (C-4'/8'), 112.1 (C-3/5,3"/5"); HRMS (EI), *m/z* Calcd for $C_{24}H_{14}N_4O_8$ (M) $^{\bullet+}$486.0812, found 486.0863.

4.1.12. 4-(1,3-dioxoisoindolin-2-yl)amino)benzoic acid (12): The data given in [18].

4.1.13. 4-((5,6-Dichloro-1,3-dioxoisoindolin-2-yl)amino)benzoic acid (13)

Yellow amorphous powder (68%); mp >300 °C ; ^{1}H NMR (700 MHz, DMSO-d_6): δ 12.50 (br s, 1H, -COO<u>H</u>), 9.18 (br s, 1H, -NH), 8.31 (s, 2H, H-4'/7'), 7.78 (d, J = 8.8 Hz, 2H, H-2/6), 6.87 (d, J = 8.8 Hz, 2H, H-3/5); ^{13}C NMR (175 MHz, DMSO-d_6): δ 167.5 (C-7), 165.1 (C-1',3'), 150.9 (C-4), 138.3 (C-5'/6'), 131.4 (C-2/6), 130.2 (C-3'a/7'a), 126.3 (C-4'/7'), 122.2 (C-1), 111.9 (C-3/5); HRMS (EI), *m/z* Calcd for $C_{15}H_8Cl_2N_2O_4$ (M) $^{\bullet+}$349.9861, found 249.9901.

.

4.2. Biology

4.2.1. In-vitro cell cultures and MTT cytotoxicity assay

The detailed methodology was reported by Abuelizz et collaborators [4]. All experiments were conducted in triplicate and repeated on three different days. All values are represented as mean ± SD. IC_{50} values were determined by Probit analysis by SPSS Inc Probit analysis (IBM Corp., Armonk, NY, USA).

4.2.2. Hoechst 33258 nuclear staining

The hoechst nuclear staining was done according to the reported protocol [19]. In brief, MCF-7 cells were seeded in 12-well plates (1×10^5 cells/well) and incubated with the IC_{50} values of compounds **7**, **9** and **10** (25, 26 and 23.5 µM, respectively) for 24 h. Cells were then washed twice with cold phosphate-buffered saline (PBS), fixed with 4% paraformaldehyde, permeabilized by cold methanol, and stained with Hoechst 33258

(Sigma-Aldrich, St. Louis, MO, USA) for 30 min in the dark. The nuclear morphological changes of apoptotic cells were observed with a fluorescence microscope (Zeiss Axio Observer D1 Zeiss, Germany).

4.2.3. FITC annexin V / PI fluorescence analysis for apoptosis quantification

The annexin V-PI apoptosis measurement was carried out in accordance to the manufacturer's protocol (Invitrogen, CA, USA). Briefly, MCF-7 cells (1×10^6 cells/well) were treated with the IC_{50} values of compounds **7**, **9** and **10** (25, 26 and 23.5 μM, respectively) for 24 h. Thereafter, both untreated and treated MCF-7 cells were washed twice with ice-cold PBS and re-suspended in 100 μL of 1X binding buffer. To the resuspended solution, 5 μL of each FITC-annexin-V and PI were added. After 15 min incubation in the dark, a binding buffer (400 μL) was added to each tube and apoptosis was quantified by flow cytometry (Cytomics FC 500; Beckman Coulter, CA, USA) [20].

4.3. QSAR model

In the HCT-116 model, ten compounds (80%) as a training set and three compounds (20%) as tests were used for QSAR modeling. The test compounds were selected by the Diverse Molecules protocol in Discovery Studio 4.5 as the external test subset. Compounds **1**, **3**, and **10** were the chosen test compounds. In the MCF-7 model, by the same protocol, ten compounds (80%) as a training set and three compounds (20%) as tests were selected for QSAR modeling. The pTI of the compounds was calculated from pTI = -log TI. In Discovery Studio, CHARMm was chosen to assign partial charges to the ligands during the assignment of a force field. In addition, the potentials of electrostatics and van der Waals were treated as separate terms. A + le point change was employed as an electrostatic potential probe, whereas the effect of the solvent was mimic by the use of the constant of distance-dependent dielectrics. In regard to the potential of van der Waals, a 1.73 Å radius carbon atom was used as a probe. An energy grid descriptor was used to build a model of partial least squares (PLS). The Create 3D QSAR Model protocol was used to build QSAR models in Discovery Studio 4.5. For a perfect model of QSAR, the value of R^2 (training set regression coefficient) and Q^2 (test set regression coefficient) must be greater than 0.6

and 0.5, respectively [21, 22]. In addition, the values of the Pearson-R value must be higher than 0.5 and root mean square error (RMSE) must be less than 0.5 [23-25].

Acknowledgments

The authors wish to thank the Deanship of Scientific Research at King Saud University for funding this work through the research group No. RG-1435-068.

References

[1] R. Al-Salahi, M. Marzouk, A. Ashour, I. Alswiadan, Synthesis and antitumor activity of 1,2,4-triazolo[1,5-a]quinazolines, Asian J. Chem., 26 (2014), 2173-2176.

[2] R. Al-Salahi, I. Alswaidan, M. Marzouk. Cytotoxicity evaluation of a new set of 2-aminobenzo[de]iso-quinoline-1,3-diones, Int. J. Mol. Sci. 15 (2014), 22483-22491.

[3] H.A. Abuelizz, M. Marzouk, H. Ghabbour, R. Al-Salahi, Synthesis and anticancer activity of new quinazoline derivatives, Saudi Pharm. J. 25 (2017), 1047-1054.

[4] H.A. Abuelizz, M.A. Hanem, M. Mohamed, F.A. Nasr, A.S. Alqahtani, A.H. Bakheit, A.M. Naglahgh, R. Al-Salahi, Synthesis and biological evaluation of 4(1H-1,2,4-triazol-1-yl)benzoic acid hydrids as anticancer agents, RSC Adv. 9 (2019), 19065–19074.

[5] R. Al-Salahi, M. E. Moustapha, H.A. Abuelizz, A.I. Alharthi, K.A. Alburikan, I.T. Ibrahim, M. Marzouk, M.A. Motaleb, Radioiodination and biodistribution of newly synthesized 3-benzyl-2-([3-methoxybenzyl]thio)benzo[*g*]quinazolin-4-(3*H*)-one in tumor bearing mice, Saudi Pharm. J. 26 (2018), 1120-1126.

[6] H.A.M. El-Sherief, B. G. M. Youssif, S. N. Abbas Bukhari, A. H. Abdelazeem, M. Abdel-Aziz, H. M. Abdel-Rahman, Synthesis, anticancer activity and molecular modeling studies of 1,2,4-triazole derivatives as EGFR inhibitors, Eur. J. Med. Chem. 156 (2018), 774-789.

[7] R. Al-Salahi, A. Ashour, M. Marzouk, K. Ashok, *In Vitro* Cytotoxicity Evaluation of a New Series of Benzo[*g*] [1,2,4]triazolo[1,5-α]Quinazolines, Latin Amer. J. Pharm. 34 (2015), 1926-1930.

[8] R. Al-Salahi, R.A. El Dib, M. Marzouk, Synthesis and *in vitro* cytotoxicity evaluation of new 2-thioxo-benzo[*g*]quinazolin-4(3*H*)–onederivatives, Heterocycles 91 (2015), 1735-1751

[9] J.F. Bereznak, D. M.-T. Chan, D. Geffken, M.A. Hanagan, G .E. Lepone, R.J. Pasteris, S.L. Swann, Preparation of fungicidal tricyclic 1,2,4-triazoles, WO 2008103357 (2008), A1 20080828**.**

[10] H.A. Abuelizz, E.H. Anouar, R. Ahmad, N.I. N. Azman, M. Marzouk, R. Al-Salahi, Triazoloquinazolines as a new class of potent α-glucosidase inhibitors: in vitro evaluation and docking study, PLoS One 14 (2019), e0220379.

[11] H. A. Abuelizz, R. A. El-Dib, M. Marzouk, R. AlSalahi, In vitro evaluation of new 2-phenoxy-benzo[g][1,2,4]triazolo[1,5-a]quinazoline derivatives as antimicrobial agents, Microb Pathog. 117 (2018), 60-67.

[12] A.A. Almehizia, H.A. Abuelizz, H.A. Taie, A. E.H. Anouar, M. Marzouk, R., Al-Salahi, Investigation the antioxidant activity of benzo[g]triazoloquinazolines correlated with a DFT study, Saudi Pharm. J. 27 (2019), 133-137.

[13] R. Al-Salahi, E.H. Anouar, M. Marzouk, H.A. Taie, H.A. Abuelizz, Screening and evaluation of antioxidant activity of some 1,2,4-triazolo[1,5-a]quinazoline derivatives, Future Med Chem. 10 (2018), 379-390.

[14] R. AlSalahi, K.E. El-Tahir, I. Alswaidan, N. Lolak, M. Hamidaddin, M. Marzouk, 2014. Biological effects of a new set 1,2,4-triazolo[1,5-a]quinazolines on heart rate and blood pressure, Chem. Cent. J. 8(1), 3.

[15] R. Al-Salahi, M. Marzouk, G. Awad, M. Al-Omar, E. Ezzeldin, Antimicrobial activity of newly synthesized methylsulfanyl-triazoloquinazoline derivatives, J. Pharm. Pharmacol. 64 (2013), 1678–1687.

[16] R. A. Al-Salahi, M. S. Marzouk, W. I. El-Eraky, D. O. Saleh, Antihistamine Activity of a new set 1,2,4-triazolo[1,5-a]quinazolines, Asian J. Chem. 26 (2014), 8625-8627.

[17] R. AlSalahi, M. Marzouk, A. Gamal Eldeen, A. Alanazi, M. Al-Omar, M. Fouda, Cytotoxic and Anti-inflammatory Active Methylsulfanyl-triazoloquinazolines, J. pure appl. Microb. 7(2013), 189-198.

[18] G. John, L. Xianfeng, L. Haixia, N. Isabel, Q. Zongxing, S. Virginie, T. Guozhi, w. Guolong, Preparation of pyridazinone-based broad spectrum anti-influenza drugs. WO 2018001948 (2018)A1 20180104.

[19] B. Chazotte, Labeling nuclear DNA with hoechst 33342." Cold Spring Harb Protoc.1 (2011) doi:10.1101/pdb.prot5557.

[20] S. Alqahtani, F.A. Nasr, O.M. Noman, M. Farooq, T. Alhawassi, W. Qamar, A. El-Gamal, Cytotoxic Evaluation and Anti-Angiogenic Effects of Two Furano-Sesquiterpenoids from Commiphora myrrh Resin, Molecules 25 (2020), 1318.

[21] A. Golbraikh, A. Tropsha, Beware of q2 J. Mol. Graph, Model, 20 (2002), 269-276.

[22] Y. Li, Y. Wang, Zhang, Pharmacophore modeling and 3D-QSAR analysis of phosphoinositide 3-kinase p110α inhibitors, J. Mol. Model. 16 (2010), 1449-1460.

[23] S.L. Dixon, A.M. Smondyrev, E.H. Knoll, S. N. Rao, D.E. Shaw, R.A, Friesner. PHASE: a new engine for pharmacophore perception, 3D QSAR model development,

and 3D database screening: 1. Methodology and preliminary results, J. Comput-Aid. Mol. Des. 20 (2006), 647-671.

[24] S.L. Dixon, A.M. Smondyrev, S.N. Rao, PHASE: a novel approach to pharmacophore modeling and 3D database searching. Chem. Biol. Drug Des. 67 (2006), 370-372.

[25] M. Tenenhaus, V.E. Vinzi, Y.-M. Chatelin, C. Lauro, PLS path modeling. Comput. Statis. Data Anal. 48 (2005), 159-205.

Highlights

- A series of 4-Hydrazinylbenzoic derivatives were synthesized.

- All derivatives were evaluated for *in vitro* anticancer activity against HCT-116 and MCF-7 cancer cells

- The active targets 6, 7 and 9 exhibited very weak cytotoxicity on normal cells (RPE-1) and showed higher IC_{50} values against HCT-116 and MCF-7 cells in relation to doxorubicin.
- Compounds 7, 9 and 10 inhibited the proliferation of MCF-7 by the induction of apoptosis.
- The bioassay results in the regression plots generated in 3D QSAR models were in agreement and correlated with the anticancer results of the target molecules.

.

Graphical abstract

The 4-hydrazinobenzoic acid derivatives were elaborated and evaluated of their *in vitro* cytotoxicity. Compounds **7, 9** and **10** showed potent inhibitory effects against HCT-116 and MCF-7 cancer cells giving IC_{50} ranged between 21.3 ± 4.1 and 28.3 ± 5.1 µM in comparison to doxorubicin. The active targets **7** and **9** exhibited very weak cytotoxicity on normal cells (RPE-1) and inhibited the proliferation of MCF-7 by the induction of apoptosis.